Self-lubricating Ni-P-MoS_2 composite coatings

Y. He, S.C. Wang, F.C. Walsh, Y.-L. Chiu, P.A.S. Reed

PII: S0257-8972(16)30963-X
DOI: doi: 10.1016/j.surfcoat.2016.09.078
Reference: SCT 21637

To appear in: *Surface & Coatings Technology*

Received date: 3 July 2016
Revised date: 28 September 2016
Accepted date: 29 September 2016

Please cite this article as: Y. He, S.C. Wang, F.C. Walsh, Y.-L. Chiu, P.A.S. Reed, Self-lubricating Ni-P-MoS_2 composite coatings, *Surface & Coatings Technology* (2016), doi: 10.1016/j.surfcoat.2016.09.078

Self-lubricating Ni-P-MoS_2 composite coatings

Y. He,[a] S.C. Wang,[a*] F.C. Walsh,[a] Y.-L. Chiu[b] P.A.S. Reed[c]

[a] National Centre for Advanced Tribology at Southampton (nCATS), University of Southampton, SO17 1BJ, UK.

[b] Department of Metallurgy and Materials, University of Birmingham, B15 2TT.

[c] Engineering Materials and Surface Engineering, University of Southampton, SO17 1BJ, UK.

Abstract: Tribological coatings with low coefficients of friction are in high demand by various industries since they can improve machine efficiency and have an environmental impact. A self-lubricating Ni-P-MoS_2 composite coating has been successfully deposited on a mild steel substrate by electrodeposition. The effects of MoS_2 on the tribological coatings have been investigated. Compared to a pure Ni-P coating, the Ni-P-MoS_2 composite coating exhibited a dramatic reduction in friction coefficient against a bearing steel ball from 0.45 to 0.05. Examination and analysis of the worn surfaces and wear debris, the composite coating showed minimum wear and oxidisation compared to the severe wear and oxidation observed in the pure Ni-P coating. The evolution of MoS_2 particles in sliding wear has been elucidated.

Keywords: self-lubrication, electrodeposition, MoS_2, Ni-P, tribofilm.

* Corresponding author:

E-Mail address:wangs@soton.ac.uk (S.C. Wang)

1. Introduction

Hard chromium coatings, with wide applications in aircraft, automotive, marine and electronics sectors, have become restricted due to the hexavalent chromium in the electrolyte which may cause severe health and environmental problems. Alternative Ni-based coatings such as Ni-Co, Ni-P and Ni-Co-P, also formed by electrochemical reduction, have shown high hardness and good wear resistance and can be considered as a potential substitute to hard chrome [1-2].

Tribological coatings with low coefficients of friction (COF) are in high demand by various industries since they can improve machine efficiency and have an environmental impact by reducing greenhouse gases (e.g., CO_2) as well as carcinogens (e.g., NO_2). Reducing the COF of Ni-based coatings, which is currently 0.4-0.7 against steel under dry lubrication, has been under continuous pursuit over the last decade. Layered materials like molybdenum disulphide (MoS_2) or tungsten disulphide (WS_2) are widely used as solid lubricants or as additives in liquid lubricants [3,4]. Their low friction performance is typically associated with easy shearing of the weak interlayer bonds (van der Waals) in these materials. WS_2 has good thermal stability up to 594°C but MoS_2 has better lubrication properties (COF as low as 0.01 in vacuum). Such an extremely low lubricant can operate somewhat like an oil medium by the formation of a tribofilm between two mutually sliding surfaces. They show an extremely low coefficient of friction due to the layered structures bonded by weak van der Waal's forces facilitating interplanar shear [3-6]. However, these solid lubricants are limited to apply in vacuum. They are less successful in humid atmospheres since water vapour and oxygen can lead to the formation of oxides which result in an increase of friction [3]. The layered lubricant has reactive dangling bonds on the prismatic edges which are susceptible to oxidise and then lead to the degradation of the low friction property. For example, MoS_2 has a low COF under 0.1 in vacuum or inert atmospheres but will rapidly increase to 0.3 in humid air. The increase of friction corresponds to the transformation of MoS_2 to MoO_3 which then disrupts layer movement [4].

The field of particle inclusion into electrodeposits by the combination of electrophoretic deposition has been comprehensively reviewed [5,6]. Successful studies of the codeposition of solid lubricants into a nickel matrix, include Ni-Co-MoS_2 [3], Ni-MoS_2 [7], Ni-W-MoS_2 coatings [8] and Ni-WS_2 [9]. With MoS_2 particle inclusions, Ni-Co composite coatings showed a reduced COF of 0.15-0.23 under loads of 1-4 N in contrast to 0.35-0.53 in the absence of a solid lubricant [3]. Cobalt salts, such as the dichloride and sulphate, however have been categorized as 'substances of very high concern' [10]. Electroplating of cobalt-based coatings is likely to face stricter regulation in the future. In other composite coatings, a high volume of MoS_2 particles have been incorporated, e.g., 20% wt. MoS_2 particles were embedded in a Ni matrix [7] and 40% in Ni-W [8]. These composite coatings had a high surface roughness and showed irregular sponge-like structures with large pores. The resultant, loose coatings could easily be wiped away and the increase in MoS_2 content did not result in low friction [8].

Ni-P alloys possess many advantages over other Ni-based coatings including higher hardness and wear resistance [11,12]. Although Ni-P coatings are amongst the very few candidates to reach 1000 HV which may indicate they can be a potential replacement for hard chrome, there are few reports on the preparation of Ni-P-MoS_2 by electrodeposition. The only reported Ni-P-MoS_2 coatings were prepared by electroless deposition, with the unstable COF valued from 0.1 [13] to 0.8 [14]. However, the high bath temperature (85°C) and unstable chemicals required by this approach would present a hostile working environment. The present research aims to develop a near frictionless and robust coating at lower bath temperature by electrodeposition. As one of few coating matrices reaching a Vickers hardness of 1000, Ni-P is an ideal candidate for a hard coating. MoS_2 particles acting as a lubrication reservoir will be incorporated into a robust Ni-P coating as well as be protected from oxidation. This self-lubricating coating will use less or do not require oil-based lubricants which is expected to attract considerable research and commercial interest.

2. Experimental details

2.1 Preparation of Ni-P-MoS_2 coatings

The coatings were deposited on a planar, 3 mm thick mild steel substrate which was polished using 120 and 800 grit silicon carbide papers, washed with detergents to remove any oil residue, dried with a paper towel then activated in 10% wt/vol hydrochloric acid for 10 seconds to remove any oxide films and to obtain an active fresh surface. The substrate was rinsed in purified water before electrodeposition. This pre-treatment ensured a good adhesion between the coating and the substrate [15].

The substrate was placed in an electrolyte solution with the compositions shown in Table 1. Each ingredient was added in sequence until fully dissolved in an ultrasonic water bath. The coatings were electrodeposited for 45 minutes at 60 ˚C. The low current density of 2.5 A dm^{-2} was chosen as the studies showed the higher current would induce cracks [16]. A PTFE-coated, cylindrical steel magnetic follower of 6 mm diameter and 25 mm length, centrally located at the bottom of an 80 mL cylindrical glass beaker was rotated at 120 rev min^{-1}. The vertically mounted, plane parallel electrodes of 4 cm^2 exposed area were immersed 25 mm apart in the bath.

2.2 Characterization of Ni-P-MoS_2 coatings

The composition of the coatings was determined using an energy dispersive spectrometer (EDS) in a JEOL JSM-6500 scanning electron microscope (SEM). The 3D surface topographies were constructed by a stand-alone software package MeX from the three tilted (+5°, 0°, -5°) secondary electron images (SEI). The phase identifications were carried out using a Bruker D2 PHASER X-ray diffractometer with Cu-Kα radiation at a scanning rate of 0.02° per second in the 2θ ranges from 10° to 80°. The hardness of the composite coatings was measured by a Vickers' micro hardness instrument (Matsuzawa MHT-1) at an applied load of 100 g for 15 s. Reported values were averaged from 5 measurements.

A reciprocating TE-77 tribometer (Phoenix, UK) was used to evaluate the friction behaviour in laboratory air with a relative humidity of 40-50% at 25 °C. The counter body was an AISI-52100 bearing steel ball (diameter 6 mm) with a hardness of 700 HV. The tests were carried out under a load of 14 N (initial Hertzian contact pressure of 1.6 GPa), a sliding frequency of 1 Hz and a sliding stroke of 2.69 mm. The frictional force was recorded automatically by a piezoelectric transducer. The depth of wear tracks were measured from the 3D Mex profiles. To clarify the lubrication function of MoS_2, a cross-section from the wear track was prepared by focused ion beam (FIB) and observed under the TEM.

A FEI Quanta 3D FIB was used to precisely mill and cut the cross-section samples from the worn area of coating. A trench depth of 15 μm was produced on either side of the area of interest and the sample was thinned to approximately 100 nm. A glass needle and a micromanipulator were used to hold the membrane and the final specimen was transferred onto a TEM grid with a Pt film. High resolution TEM (HRTEM) images were obtained from a JEOL JEM 3010 operating at 300 kV with a resolution of 0.21 nm.

3. Results

3.1 The effect of MoS_2 concentration on surface morphology

The as-received MoS_2 particles are irregular with the majority having a size of 1-4 μm, as shown by SEI in Fig. 1a). The pure Ni-P coating retained the as-received substrate morphology (Fig. 1b) which indicated the coating grew homogenously. In contrast, the Ni-P-MoS_2 coatings in Figs. 1c)-f) had rough surfaces with nodules. The inhomogeneities are believed to be due to the preferential deposition of Ni atoms on the conductive surfaces of the MoS_2 particles once these were attached on the cathode substrate, instead of Ni atoms depositing homogeneously on the substrate. At a low level of MoS_2 particles (i.e. a concentration of 2%), the corresponding coating in Fig. 1c) shows a rougher surface, which is due to the low nucleation sites and subsequently growing to individual large crystals. With the increase of the MoS_2 incorporation, the composite coatings in Fig. 1d)-f) have much smoother surfaces with growth of smaller crystals. This indicates that the incorporated MoS_2 could be the sites for the nucleation of nickel growth. The increase of MoS_2 in the bath electrolytes led to the formation of more dense structures. This has been further evidenced by the 3D surface morphologies constructed by MEX in Fig. 2. The composite coating of 2%

MoS_2 had some large peaks and troughs of the order of tens of microns in Fig. 2a). With the increase of MoS_2 particle content to 7.9%, the coating surface became almost flat in Fig. 2c). This effect can be understood by appreciating that more nucleation sites on the Ni-P would be available at higher MoS_2 concentration and the roughness was reduced. A further increase of MoS_2 concentration (20 g L^{-1}) led to a slightly rougher surface in Fig. 2d). The average surface roughness (S_a) varies from 8.9 μm (with 2% MoS_2), 4.6 μm (with 4.1% MoS_2), 2.0 μm (with 7.9% MoS_2) to 2.9 μm (with 7% MoS_2) as summarized in Fig. 3a). The content of MoS_2 particles incorporated in the coatings versus the concentration of particles added in the electrolytes is shown in Fig. 3b). A linear relationship held up to 10 g L^{-1} in the bath electrolyte. However after this, little change was observed with a further increase in the bath concentration, e.g. 20 g L^{-1}, which might be due to the concentration saturation causing the particles' aggregation [17].

XRD was employed to study the texture and phase structure of the Ni-P-MoS_2 coatings as shown in Fig. 4. The broad peaks around 45° which appeared in all the coatings were attributed to {111} plane of the Ni phase. The dominant {111} plane in all deposits was associated with the low surface energy of this plane during electrodeposition. A small Ni {220} peak at 76° existed in the Ni-P coating but disappeared for the Ni-P-MoS_2 coatings. This could be because in the composite coatings the Ni preferred to nucleate around the MoS_2 particles rather than the Fe/Ni matrix. The crystal size of the Ni-P matrix was calculated by the Scherrer equation using Ni {111}. The crystal size has been estimated as 2.7 nm for the Ni-P coating and as 1.8 nm for the coatings with MoS_2 addition (regardless of MoS_2 concentration). This refinement is attributed to the adsorption of nanoparticles on the cathode which act as nucleation sites for Ni deposition and growth [18,19]. On the other hand, the particles increase the charge-transfer resistance of the electroplating processes and therefore cause a more negative cathodic potential which enhanced the crystal refinement. The peaks located at 14°, 33°, 36°, 39° and 50° are consistent with the standard peaks of hexagonal MoS_2 (JCPDS Card number 00-024-0513). Stronger XRD peaks corresponded to higher levels of MoS_2 in the coatings.

3.2 The effect of MoS_2 contents on friction

The Vickers hardness test was conducted using a diamond tip micro-indenter and the value

was calculated from indentation widths. However, due to the rough surface of the samples, it was difficult to obtain clear indentation marks. Nano-indentations were carried out on the cross-section of the coatings to acquire more reliable values of hardness. All the Ni-P-MoS_2 coatings showed improved hardness in a range of 605 to 627 HV compared to the Ni-P coating at 530 ± 60 HV (Fig. 5a). As MoS_2 is much softer than Ni-P, the hardness increase of the composite coating must be attributed to other factors, particularly the decreased crystal sizes from 2.7 nm to 1.8 nm, where the increased grain boundaries may hinder dislocation mobility.

Fig. 5b shows the friction coefficients versus time produced by the Ni-P and Ni-P-MoS_2 composite coatings against the steel ball. The friction coefficient of the Ni-P coating fluctuated but was relatively stable at 0.45. In contrast, the friction coefficients of all composite coatings are much lower. The friction coefficients of the 2.0% wt., 4.1% wt. and 7.1% wt. MoS_2 embedded coatings started at 0.1 and ended at 0.3, 0.2 and 0.1 respectively at the end of 1000 seconds reciprocating slide. While MoS_2 increased to 7.9% wt. of the coating, the coefficients of friction exhibited a steady low friction coefficient of 0.05 over 1000 s. In order to test the durability of this coating, an extended, 1 hour reciprocating test was carried out. The coating maintained the low friction without any sign of particle degradation [16].

3.3 MoS_2 contents on wear of the coatings and counterpart balls

After a 1000 s wear test, the morphology of wear tracks on the substrate was imaged under SEI. Grooves and scars along the sliding direction were observed on the wear track of Ni-P in Fig. 6a, which indicated that severe adhesive wear occurred. The wear tracks on the Ni-P-MoS_2 coatings showed polished surfaces in Figs. 6b-e which were distinctly different from Fig. 6a. With the increase of the particle content, the width of the wear track decreases. The Ni-P-MoS_2 7.9% wt. coating shows one-third the width of wear track compared to the 2% wt. MoS_2 inclusion coating. The compositions of the wear tracks were measured as listed in Table 2. In the Ni-P coating without MoS_2 incorporation, a high level of oxygen (9.8%) was detected. This indicated a severe oxidation occurred on the coating during the testing. The presence of a few percentage of iron was wear transfer from the counterpart bearing steel ball. On the 2% wt. MoS_2-Ni-P coating, the oxidised debris of MoO and/or NiO were formed and

are presumed responsible for the COF rise to 0.3. With a further increase to 4.1% wt. MoS_2, the patches width was narrower (Fig. 6c) and the oxidation was reduced significantly and a low coefficient of friction was achieved. The oxidation was further suppressed in the 7.9% wt. MoS_2-Ni-P coating sliding against steel. These patches were a MoS_2 containing tribofilm confirmed by EDS. However, with the further increase of the MoS_2 concentration, the oxidation of the 7.1% wt. MoS_2-Ni-P coating rose again as well as coefficient of friction. The increase of the MoS_2 concentration in the solution could result in the aggregation and as a consequence reduce the effective MoS_2 coverage in the coating. This resulted in an increase of the friction coefficient.

The wear tracks on the counterpart steel balls were also investigated using SEM. After sliding against the Ni-P coating, the counterpart steel ball formed a rough disc with number of debris pieces as shown in Fig. 7a). The was in micron sizes with the compositions dominated by Ni-P as listed in Table 3. This indicated the coating debris was transferred to the counterpart ball, which is understandable as the hardness of the counterpart ball (700 HV) is harder than the Ni-P coating (530 HV). Against the 2% wt. MoS_2-Ni-P coating, the counterpart ball had a similar wear scar but finer sized debris as shown in Fig. 7b). The debris also consisted of MoS_2 in addition to Ni-P, and Fe_xO_y. Sliding against the 7.9% wt. The counterpart balls possessed higher O contents than that of pure Ni-P as the rough structure of the coating generated high pressure against each other and thus caused frictional heat and severe oxidation. When the contents of MoS_2 in the coatings increased further, the surface roughness decreased and thus the oxidation on the counterpart balls also decreased. Sliding against the 7.9 wt.% MoS_2-Ni-P coating, the EDS analysis showed that the steel ball consisted of mostly Fe and few O. The corresponding ball's surface in Fig. 7c) had much less debris with a dark appearance. These patches were dominated by Ni, P and MoS_2, which were transferred from the coating. Considering the percentage of MoS_2 over (Ni-P+MoS_2) was 40% compared to 7.9% on average in the coating, it may be concluded that MoS_2 was more readily transferred than Ni-P onto steel to form a tribofilm layer acting as lubrication.

Fig. 8a shows the embedded MoS_2 particles appear as a slight darker colour in the backscattered electron (BSE) mode. Observations of the cross-sectional BSE images of Ni-

P/MoS_2 composite coatings confirm that the content of the MoS_2 particles in the composite coatings increased substantially as the particle loading in the plating solution increased from 1 to 10 g L^{-1} but almost unchanged with a further increase of the particle concentration to 20 g L^{-1}. A FIB-SEM system was used to examine the cross-section of the wear track to identify further the behaviour of MoS_2 particles in the wear process. The ball-on-flat wear testing was carried out in the Ni-P-7.9%MoS_2 coating under a load of 14 N for 1000 seconds. The cross-section was lifted up in FIB. The backscattered SEM image (centre) and high resolution TEM micrographs (two in left and one in bottom) were taken as shown in Fig. 8b. The top edge in the SEM image provides a side view of the coating surface. In the coating the greyer areas were confirmed as MoS_2 by EDS in TEM. Within 2 microns of the worn surface, MoS_2 particles were elongated from irregular in the as-received particles. Each elongated direction was observed parallel to its *c* plane i.e. $(002)_{MoS2}$ although this might deviate a few degrees only from the worn surface, as shown by high resolution TEM, e.g. I and II. With the further depth of 2-3 microns away from the surface, a large MoS_2 particle was split into pieces by shear stress. All of these parts were elongated along $(002)_{MoS2}$ although not aligned to the worn surface, e.g. III & IV. It is interesting to observe that the majority of these split parts were arranged in a triangle with or without contacts directly. Such a pattern was well recognised in the hexagonal titanium from phase transformation, and had been attributed to self-accommodation in order to minimise the transformation strain [20]. It is reasonable to deduce that such an arrangement of these fractured MoS_2 could act in a similar way to accommodate the strain induced due to the shear applied [21].

4. Discussion

During metal or alloy electrodeposition, the distribution of current over the smooth surface of electrodes is uniform, all the metal ions moving in the electrolyte being subject to the same Coulomb force E^*q_t (E represents the electric field, q_t represents the charge of ions) [22, 23]. The deposition rate remains constant at the different sites on the substrate, therefore a homogenous coating is expected to be produced. However, the situation was different for composite electrodeposition of Ni-P-MoS_2. The change is directly related to the non-uniform distribution of current on the electrode surface with adsorbed particles. When conductive or

semi-conductive particles were added into the electrolytic solution, the electrolytic current concentrated in the vicinity of particles on the cathode (bigger E) as illustrated in Fig. 9. In consequence, the ions in solution move at higher velocity υ towards these tip points due to the greater Coulomb force E^*q_t , speeding up the crystal growth at these locations and creating many deposit protrusions on the surface. As a result, a rough surface was obtained for the Ni-P-MoS_2 coating while the Ni-P coating displayed a flat surface.

MoS_2 has been attracted intensive interest as a solid lubricant. However, in a humid environment, MoS_2 is easily oxidized to MoO_3 which can cause the material to stick, accelerate the deterioration of its easy shear performance and lead to an increase of friction. In the composite coating, however, the MoS_2 particles were fully surrounded by Ni-P matrix and thus prevented from oxidizing. Accordingly these coatings can maintain a low friction coefficient for a long period. Compared to the mild steel (Fig. 10a) and the Ni-P coating (Fig. 10b), no oxidation was detected after wear against a bearing steel ball as shown in Fig. 10c). These results confirm that the solid lubricant has reduced the friction of the resultant Ni-P coating, and the higher the amount of MoS_2 incorporated in the coating the lower the friction coefficient achieved. MoS_2 has a much stronger adhesion to the Ni matrix than to a stainless steel [24], in which the strong interatomic bonding would endure the high stress and reduce wear damage. This was evidenced by the integrity of the Ni-P-MoS_2 coating during the long wear test. The weak Van der Waal's bonding between two layers allows MoS_2 to slide easily, providing low friction. A sufficient concentration of MoS_2 (7.9% wt. in this study) ensured the formation of a complete self-lubricated tribofilm to avoid the metal-metal contact, in this case, Ni-iron contact. This could explain why some previous reports of the COFs on metal-MoS_2 coatings were as high as 0.8, e.g. [14]. The integrated tribofilm was also accompanied by the benefit of diminishing oxidation by reducing heating due to friction. The tribofilm was transferred to the counterpart steel ball as lubrication therefore less frictional heat was generated and less oxidation occurred. Therefore, the increase of MoS_2 content in the coating has not only improved the wear resistance of the coating but also effectively protected the counterpart ball from wear.

5. Conclusions

The present research has successfully developed a robust coating with an extremely low friction coefficient. This composite of Ni-P-MoS_2 coating was fabricated by an advanced electro-deposition technique and can be used in harsh condition such as humid atmosphere instead of the vacuum conditions only often used for MoS_2. The friction coefficient of the 7.9MoS_2-Ni-P composite coatings sliding again steel in air exhibited a steady-state value of 0.05 during a 1-hour reciprocating test, which is almost one grade lower than that of 0.45 of the Ni-P coating without MoS_2 inclusion.

The concentrations of MoS_2 particles in the electroplating bath have significant impacts on the surface roughness as well as content of the composite coatings. In return the incorporation of MoS_2 particles in the Ni-P composite strongly influences the friction performance of coatings. Severe abrasion and oxidation wears were observed in the Ni-P coating but very rarely for the Ni-P-MoS_2 composite coating. On the Ni-P-MoS_2 (7.9% wt.) coating, uniform and compact tribofilm abundant in MoS_2 were observed on both coating surface and the counter ball, protecting the coating from oxidation. These MoS_2 were strongly adhered to the surface (Ni matrix) therefore it remains effective in lubrication rather than being squeezed out. FIB and TEM studies demonstrated that just under the wear testing pressure MoS_2 particles near the coating surface were broken into elongated fragments parallel to their *c* plane and the coating surface. The compact structure and the high content of MoS_2 are considered to be critical conditions for the electrodeposited Ni-P-MoS_2 acting a robust, low friction coating.

Acknowledgements

The work is supported by the China Scholarship Council, Faculty of Engineering and the Environment of Southampton University, the Royal Society (IE111270) and the Royal Academy of Engineering (1314RECI080). The authors would also like to thank FCW thanks EPSRC for the award of a Green Tribology research grant (EP/J001023/1).

Figure captions

Figure 1. SEI planar views on (a) as-received MoS_2 particles; (b) Ni-P coating; (c-f) Ni-P-MoS_2 composite coatings prepared by the electrolytes with different MoS_2 concentrations of 3, 7, 10 and 20 g L^{-1} respectively.

Figure 2. 3-D surface topographies of Ni-P-MoS_2 composite coatings prepared by the electrolytes with different MoS_2 concentrations of (a) 3; (b) 7; (c) 10 and (d) 20 g L^{-1}.

Figure 3. (a) The relationship of MoS_2 contents in the coatings fabricated and in the electrolytes prepared; (b) EDS measured contents of MoS_2 particles in the Ni-P composite coatings against the corresponding concentrations.

Figure 4. X-ray diffraction patterns of Ni-P and Ni-P-MoS_2 coatings.

Figure 5. (a) Vickers harnesses and (b) friction coefficients of the Ni-P and Ni-P-MoS_2 coatings.

Figure 6. SEI observations of the wear tracks on the Ni-P coatings with different MoS_2 contents of (a) 0; (b) 2 wt.%; (c) 4.1 wt.%, (d) 7.9 wt.% and (e) 7.1 wt.%

Figure 7. SEI observations of the counterpart balls after sliding test against (a) the Ni-P coating; (b) the 2 wt.% MoS_2-Ni-P coating; (c) the 7.9 wt.% MoS_2-Ni-P coating; (d) 7.1 wt.% MoS_2-Ni-P coating and (e) topography of the same location as (c).

Figure 8. (a) Backscattered SEM image of the FIB cross-sectional sample from the wear track of Ni-P-MoS_2 (7.9 wt.%) coating and (b) HRTEM images of typical MoS_2 particles with different depths of the coating.

Figure 9. A schematic diagram representing the current distribution near the electrode during the composite electrodeposition.

Figure 10. The oxygen mapping of the wear tracks on (a) substrate, (b) Ni-P coating, and (c) Ni-P-MoS_2 (7.9 wt.%) composite coating after 1000 s friction.

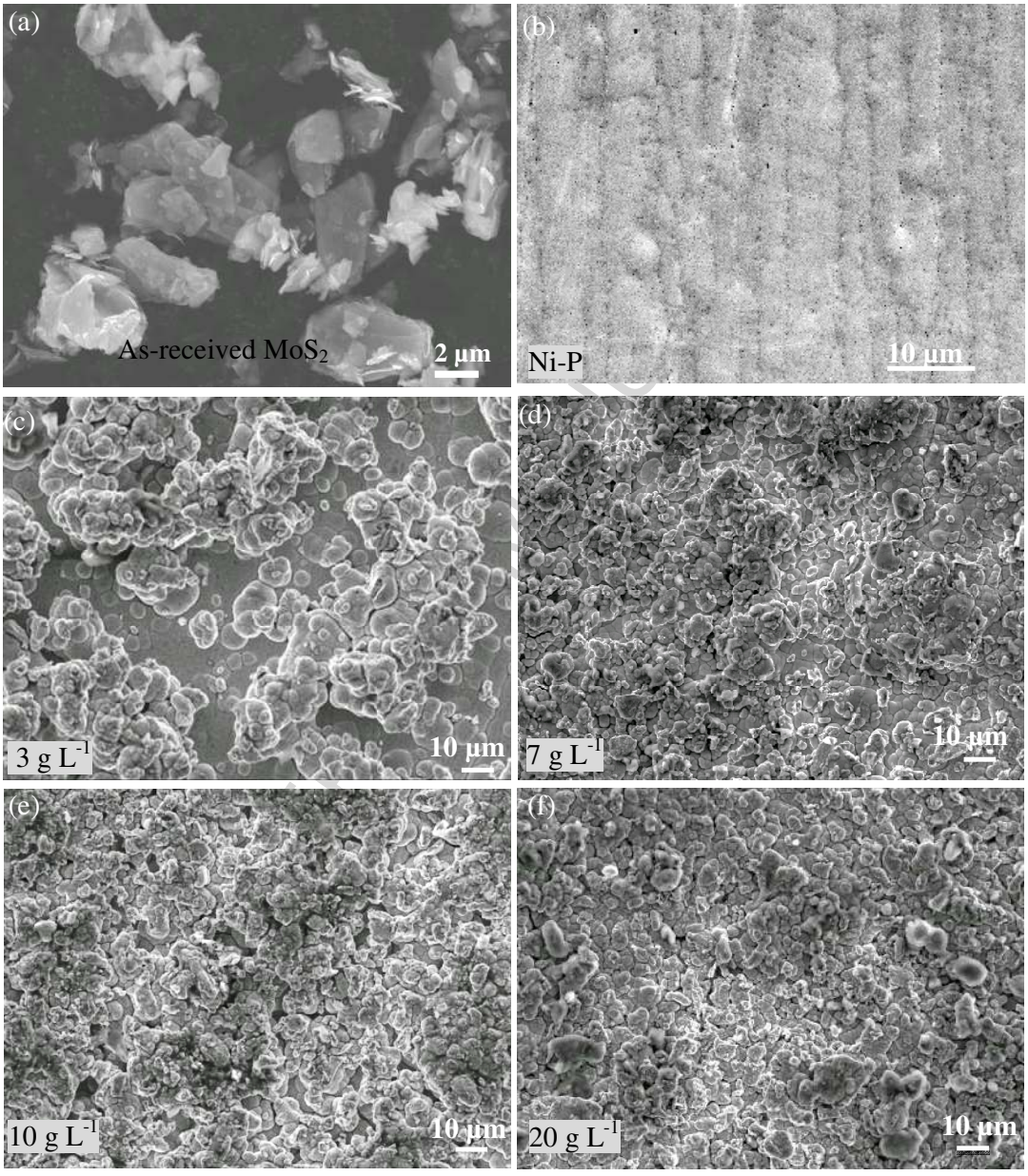

Fig. 1

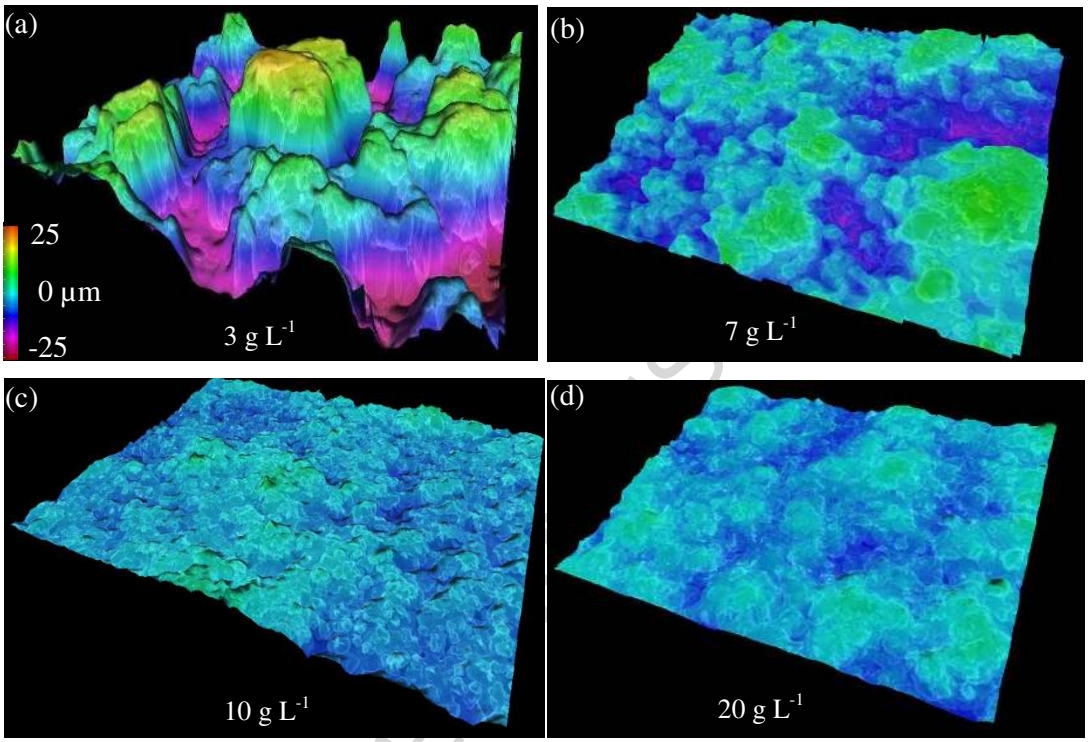

Fig. 2

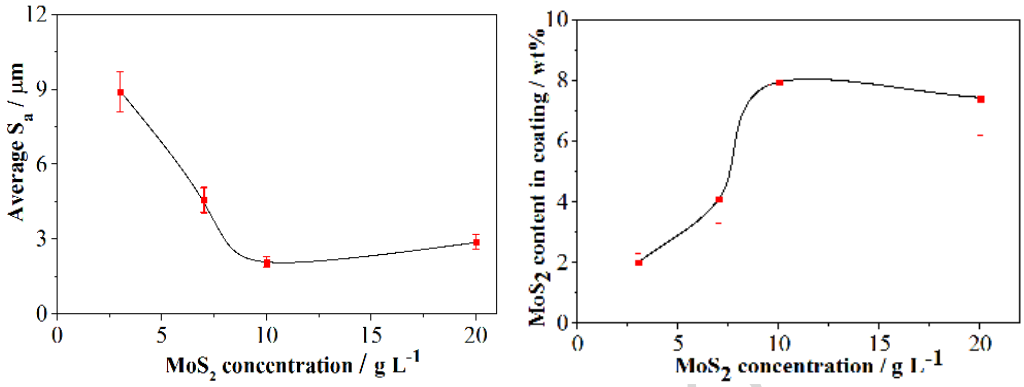

(a) (b)

Fig. 3

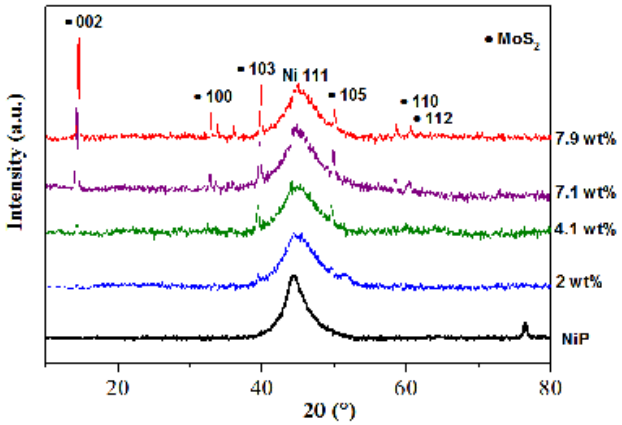

Fig. 4

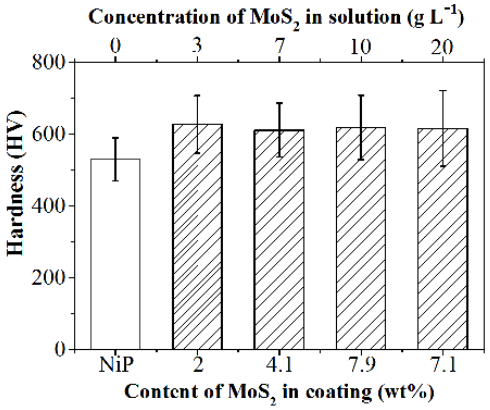

(a)

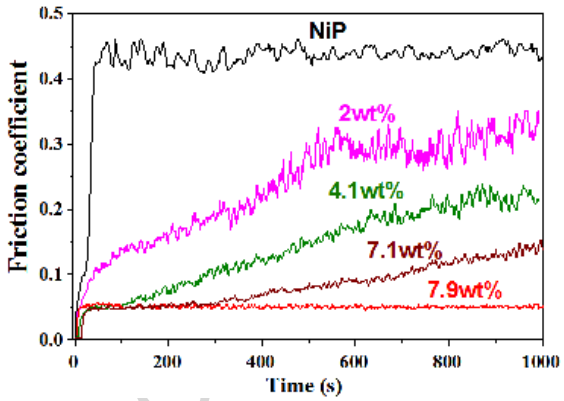

(b)

Fig. 5

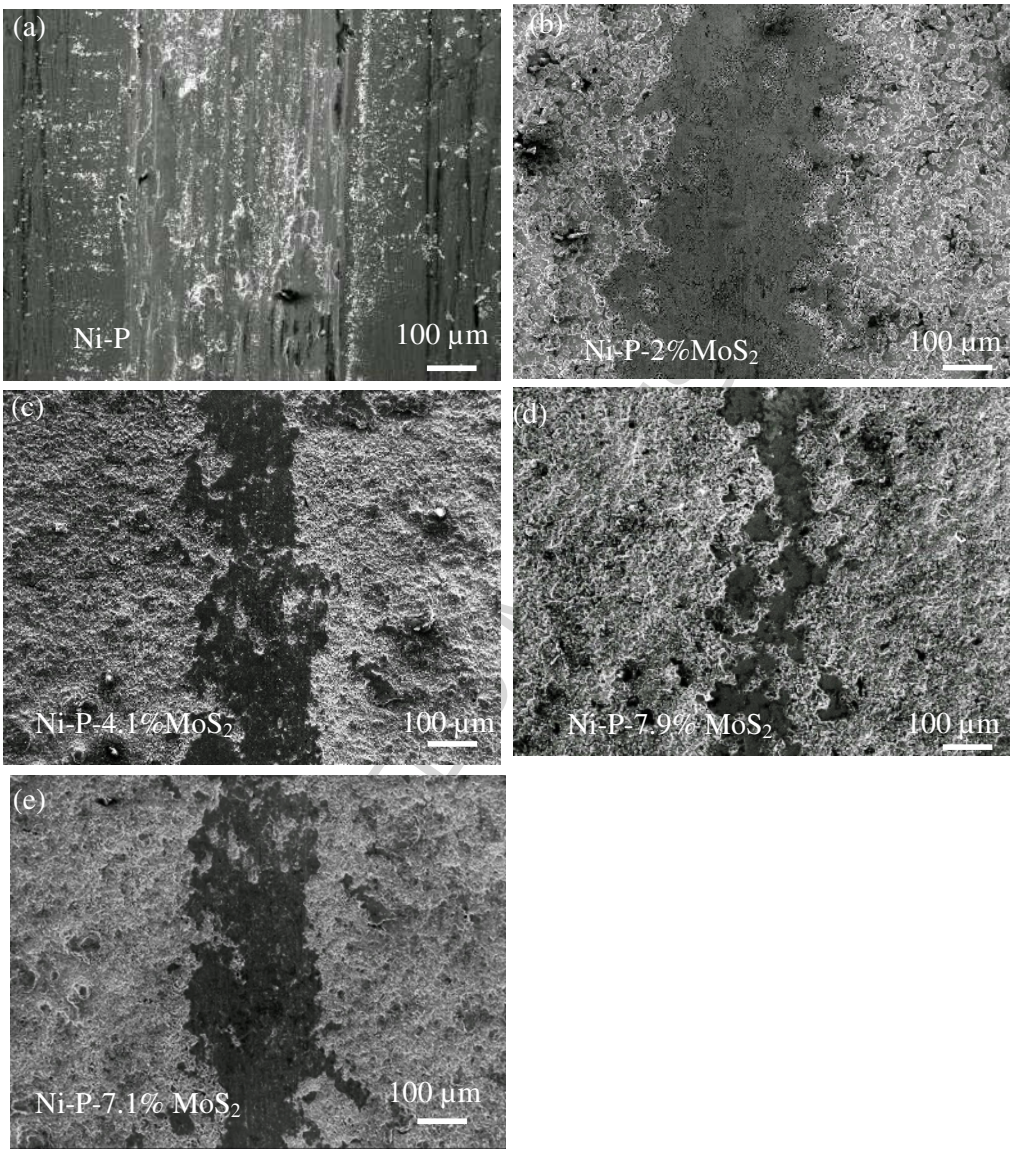
(a)
Ni-P
100 µm
(b)
Ni-P-2%MoS2
100 µm
(c)
Ni-P-4.1%MoS2
100 µm
(d)
Ni-P-7.9% MoS2
100 µm
(e)
Ni-P-7.1% MoS2
100 µm

Fig. 6

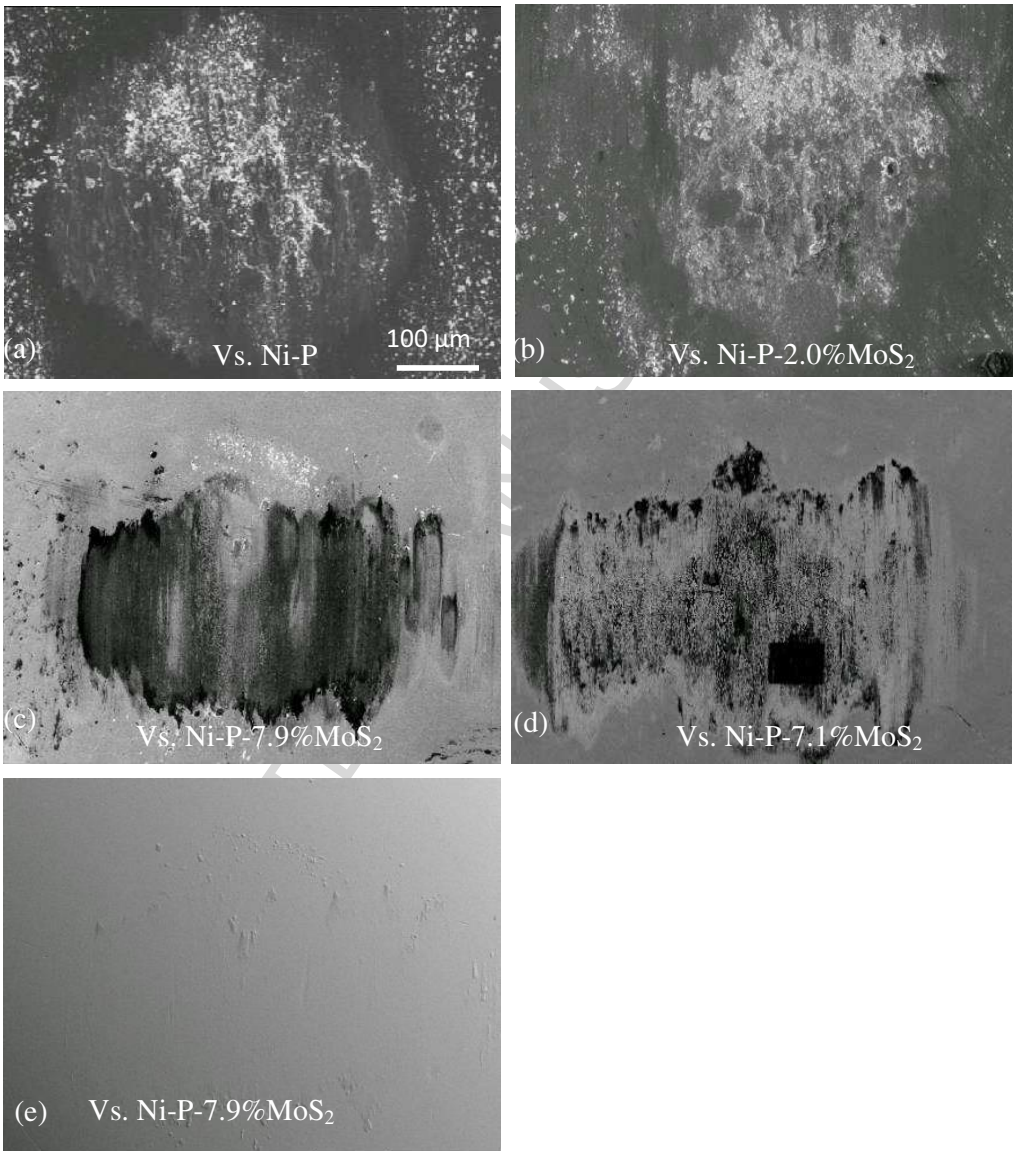

Fig. 7

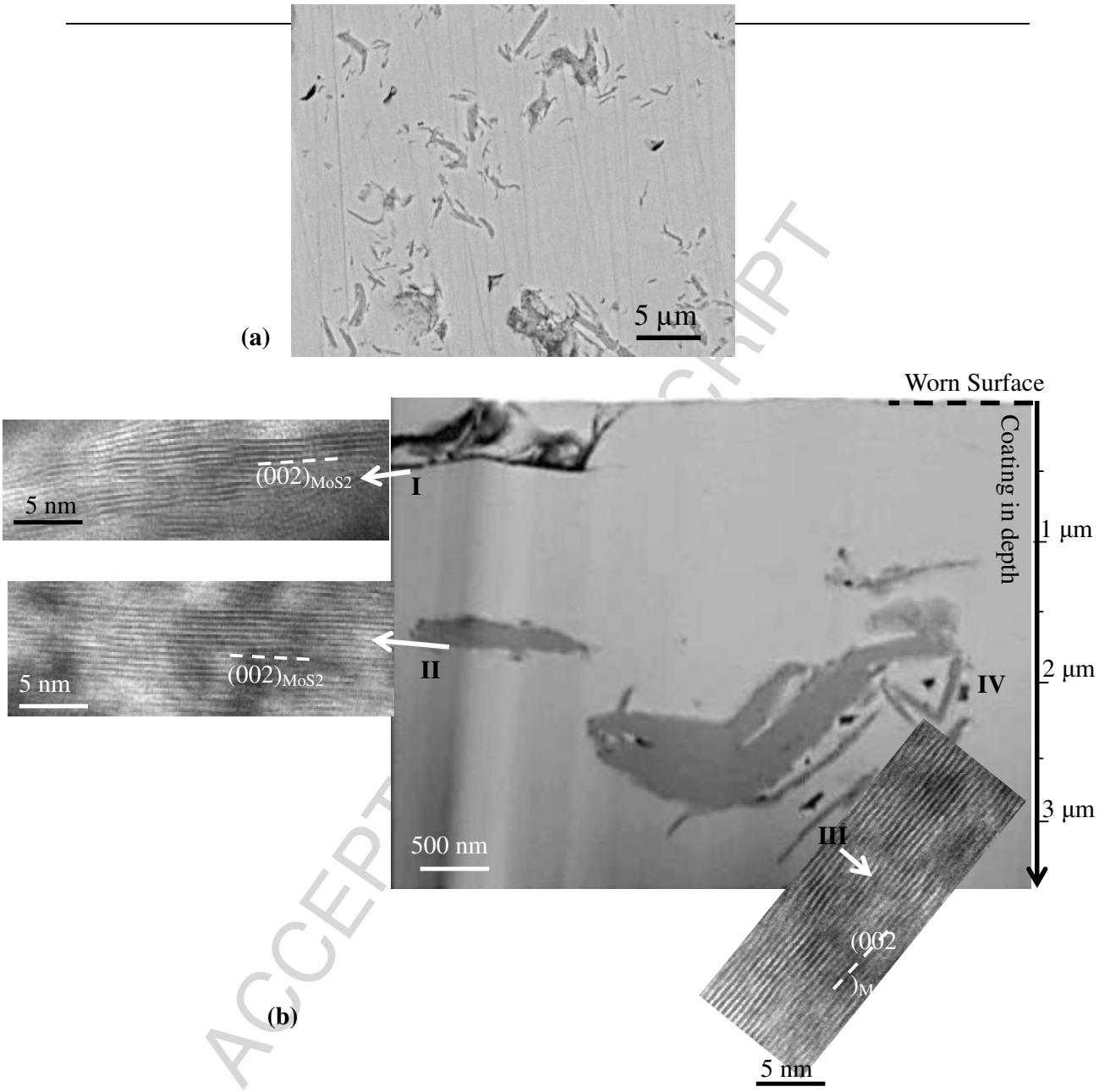

Fig. 8

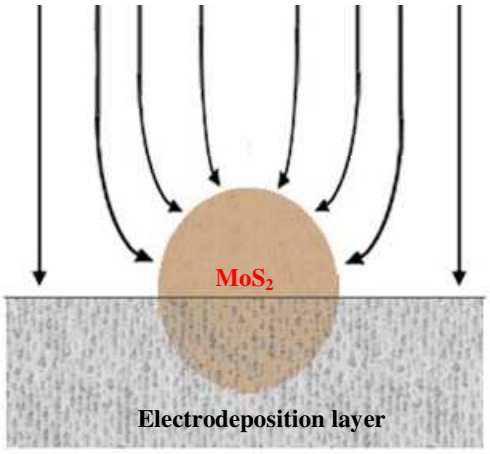

Fig. 9

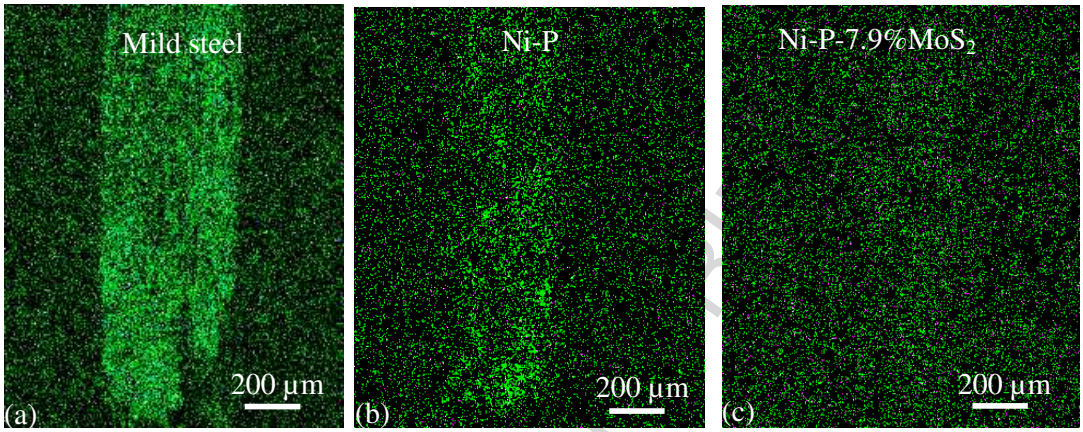

Fig. 10

Table 1. The electrolyte composition used for the Ni-P-MoS_2 deposits

Chemical compound	Concentration (g L^{-1})	Sourced from
$NiSO_4 \cdot 6H_2O$	220	Sigma-Aldrich
H_3BO_3	30	Sigma-Aldrich
NaH_2PO_2	10	Sigma-Aldrich
$NiCl_2 \cdot 6H_2O$	45	Sigma-Aldrich
$HOC(COOH)(CH_2COOH)_2$	12	Sigma-Aldrich
Cetyltrimethylammonium bromide, CTAB	0.1	Sigma-Aldrich
MoS_2	3, 7, 10, 20	Shanghai ST-Nano Science & Technology

Table 2. Chemical composition (wt.%) by EDS analysis on the wear tracks of all the coatings

Coating (wt.%)	Ni-P	MoS_2	O	Fe
Ni-P	87.9	-	9.8	2.3
Ni-P-2MoS_2	87.5	4.6	7.9	-
Ni-P-4.1MoS_2	90.1	7.8	2.1	-
Ni-P-7.1MoS_2	89.1	9.3	1.5	-
Ni-P-7.9MoS_2	87.3	12.1	0.6	-

Table 3. Chemical composition (wt.%) by EDS analysis on wear tracks of the counterpart balls after wear test against different coatings

Coating (wt.%)	Ni-P	MoS_2	O	Fe-Cr
Ni-P	51.9	-	10.1	38.0
Ni-P-2MoS_2	32.8	1.2	15.5	50.5
Ni-P-4.1MoS_2	22.6	6.3	7.2	63.9
Ni-P-7.1MoS_2	11.8	3.4	3.5	81.3
Ni-P-7.9MoS_2	3.8	2.5	2.0	91.7

Highlights

- Successfully electrodeposited a super lubricated Ni-P-MoS_2 coating.
- Composite coatings may extend the application of MoS_2 to humid atmosphere.
- MoS_2 contents have a strong influence on friction.

References

1 F.D. Torre, H.V. Swygenhoven, M. Victoria, Nanocrystalline electrodeposited Ni: microstructure and tensile properties, Acta Materialia 50 (2002) 3957-3970.

2 C. Ma, S.C. Wang, L.P. Wang, F.C. Walsh, R.J.K. Wood, The electrodeposition and characterisation of low-friction and wear-resistant Co-Ni-P coatings, Surface and Coatings Technology 235 (2013) 495-505.

3 L. Shi, C. Sun, W. Liu, Electrodeposited nickel-cobalt composite coating containing MoS_2, Applied Surface Science 254 (2008) 6880-6885.

4 J.L. Grosseau-Poussard, P. Moine, M. Brendle, Shear strength measurements of parallel MoS_x thin films, Thin Solid Films 307 (1997) 163-168.

5 J.P. Celis, J.R. Roos, C. Buelens, J. Fransaer, Mechanism of electrolytic composite plating – survey and trends, Transactions of the Institute of Metal Finishing 69 (1991) 133-139.

6 F.C. Walsh, C. Ponce de León, A review of the electrodeposition of metal matrix composite coatings by inclusion of particles in a metal layer: an established and diversifying coatings technology Transactions of the Institute of Materials Finishing 92 (2014) 83-98.

7 L.M. Wang, Effect of surfactant BAS on MoS_2 codeposition behaviour, Journal of Applied Electrochemistry 38 (2008) 245-249.

8 M.F. Cardinal, P.A. Castro, J. Baxi, H. Liang, F.J. Williams, Characterization and frictional behavior of nanostructured Ni-W-MoS_2 composite coatings, Surface and Coatings Technology 204 (2009) 85-90.

9 G. Zhao, Y. Xue, Y Huang,d Y Ye, F.C Walsh, J. Chen and S.C. Wang, One-step electrodeposition of a self-cleaning and corrosion resistant Ni/WS2 superhydrophobic surface, RSC Adv.,9 (2016) 59104-59112

10 Candidate List of Substances of Very High Concern for authorisation, in http://echa.europa.eu/web/guest/candidate-list-table. Accessed on 4th May, 2016.

11 S.M. Monir Vaghefi, A. Saatchi, M. Ebrahimian-Hoseinabadi, Deposition and properties of electroless Ni-P-B4C composite coatings, Surface and Coatings Technology 168 (2003) 259-262.

12 K. Zangeneh-Madar, S.M. Monir Vaghefi, The effect of thermochemical treatment on the structure and hardness of electroless Ni-P coated low alloy steel, Surface and Coatings Technology, 182 (2004) 65-71.

13 T.Z. Zou, J.P. Tu, S.C. Zhang, L.M. Chen, Q. Wang, L.L. Zhang, D.N. He, Friction and wear properties of electroless Ni-P- (IF-MoS_2) composite coatings in humid air and vacuum, Materials Science and Engineering A 426 (2006) 162-168.

14 Z. Li, J. Wang, J. Lu, J. Meng, Tribological characteristics of electroless Ni-P-MoS_2 composite coatings at elevated temperatures, Applied Surface Science 264 (2013) 516-521

15 Y. He, S.C. Wang, F.C. Walsh, W.S. Li, L. He, P.A.S. Reed, The monitoring of coating health by *in-situ* luminescent layers, RSC Advance 5 (2015) 42965-42970

16 Y. He, Electrodeposition of nickel-based composite coatings for tribological applications, PhD thesis, University of Southampton, December 2015.

17 E. Pompei, L. Magagnin, N. Lecis, P.L. Cavallotti, Electrodeposition of nickel-BN composite coatings, Electrochemica Acta 54 (2009) 2571-2574.

18 L. Benea, P.L. Bonora, A. Borello, S. Martelli, F. Wenger, P. Ponthiaux, J. Galland, Composite electrodeposition to obtain nanostructured coatings, Journal of the Electrochemical Society 148 (2001) C461-C465.

19 B.S.B. Reddy, K. Das, A.K. Datta, S. Das, Pulsed co-electrodeposition and characterization of Ni-based nanocomposites reinforced with combustion-synthesized, undoped, tetragonal-ZrO_2 particulates, Nanotechnology 19 (2008) 115603-115613.

20 S.C. Wang, M. Aindow, M.J. Starink, Effective of self-accommodation on α/α boundary populations in pure titanium, Acta Material 51 (2003) 2485-2503

21 S.C. Wang, Y. He, Y-L Chiu, P.A.S. Reed, F.C. Walsh, Shear-induced self-accommodation of MoS_2 in the NiP electrodeposit, to be published.

22 S. Mehdizadeh, J.O. Dukovic, P.C. Andricacos, L.T. Romankiw, H.Y. Cheh, The influence of lithographic patterning on current distribution: A model for microfabrication by electrodeposition, Journal of the Electrochemical Society 139 (1992) 78-91.

23 C. Wang, Y. Zhong, W. Ren, Z. Lei, Z. Ren, J. Jia, A. Jiang, Effects of parallel magnetic field on electrocodeposition behavior of Ni/nanoparticle composite electroplating, Applied Surface Science 254 (2008) 5649-5654.

24 G.C. Barton, S.V. Pepper, Transfer of molybdenum disulfide to various metals, NASA Technical Paper 1997: 1019.